Electronic Supplementary Information

Mechanical switching of current-voltage characteristics in spiropyran single-molecule junctions

Takashi Tamaki,[a] Keigo Minode,[b] Yuichi Numai,[b] Tatsuhiko Ohto,[b] Ryo Yamada,[b] Hiroshi Masai[a], Hirokazu Tada[b]* and Jun Terao[a]*

[a] Department of Basic Science, Graduate School of Arts and Sciences, The university of Tokyo, Tokyo 153-8902, Japan.
E-mail: cterao@mail.ecc.u-tokyo.ac.jp
[b] Graduate School of Engineering Science, Osaka University, 1-3 Machikaneyama-cho, Toyonaka, Osaka 560-0043, Japan.
E-mail: tada@molectronics.jp

Index

Experimental Section

Experimental comments, Equipment and Procedures

Materials: Unless otherwise noted, commercially available chemicals were used as received. Dry toluene and THF were purchased from Kanto Chemical and further purified by passage through activated alumina under positive nitrogen pressure as described by Grubbs et al.[1] 5-bromo-1,2,3,3-tetramethyl-3H-indol-1-ium iodide[2] and 4-bromo-2-hydroxybenzaldehyde[3] were prepared via the reported procedures.

NMR spectroscopy: ^{1}H NMR (500 MHz) and ^{13}C NMR (126 MHz) were measured with a Bruker AVANCE III HD 500 spectrometer. The ^{1}H NMR chemical shifts were reported relative to tetramethylsilane (TMS, 0.00 ppm) or residual protonated solvent (7.26 ppm for $CDCl_3$). The ^{13}C NMR chemical shifts were reported relative to TMS (0.00 ppm) or deuterated solvents (77.16 ppm for $CDCl_3$).

Preparative Recycling Gel Permeation Chromatography (GPC): Preparative recycling GPC was performed with a SHIMADZU LC-20AP System equipped with a Shodex K-4001L or Shodex K-4002.5L column, a SHIMADZU SPD-20A, and a SHIMADZU RID-10A using $CHCl_3$ as the eluent at a flow rate of 14 mL min^{-1}.

Synthesis of Br-SP-Br

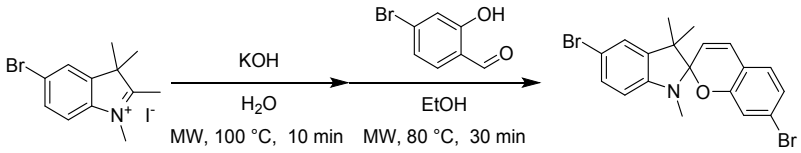

5',7-dibromo-1',3',3'-trimethylspiro[chromene-2,2'-indoline] (Br-SP-Br)

5-bromo-1,2,3,3-tetramethyl-3H-indol-1-ium iodide (214 mg, 0.56 mmol), one pellet of KOH (about 70 mg) and 1 mL of water were added to microwave vessel equipped with a magnetic stir bar. The reaction vessel was securely capped and subjected to microwave irradiation for 10 min at 100 °C. The organic compound was extracted with dichloromethane and the organic solvent was evaporated. Then, the crude compound, 4-bromo-2-hydroxybenzaldehyde (115 mg, 0.57 mmol) and 0.6 mL of ethanol were added to microwave vessel equipped with a magnetic stir bar. The reaction vessel was securely capped and subjected to microwave irradiation for 30 min at 80 °C. Organic solvent was evaporated and the crude material was purified by column chromatography (silica-gel, ethyl acetate/hexane = 9/1) and GPC ($CHCl_3$) to afford 113 mg of Br-SP-Br as white solid in 46% yield.

^{1}H NMR (500 MHz, $CDCl_3$) δ 7.26 (dd, J = 8.2, 2.0 Hz, 1H), 7.14 (d, J = 1.9 Hz, 1H), 6.96 (dd, J =

8.0, 1.8 Hz, 1H), 6.91 (s, 1H), 6.89 (t, *J* = 1.8 Hz, 1H), 6.82 (d, *J* = 10.3 Hz, 1H), 6.39 (d, *J* = 8.2 Hz, 1H), 5.67 (d, *J* = 10.2 Hz, 1H), 2.69 (s, 3H), 1.27 (s, 3H), 1.15 (s, 3H).

^{13}C NMR (126 MHz, $CDCl_3$): δ 154.8, 147.1, 138.9, 130.2, 129.0, 127.8, 124.8, 123.4, 122.6, 119.0, 118.2, 117.6, 111.1, 108.4, 104.7, 51.9, 28.9, 25.7, 19.9

HRMS-TOF(ESI): m/z calc.: 432.9677 $[C_{19}H_{17}Br_2NO]^+$, found: 432.9675.

Synthesis of RS-SP-SR

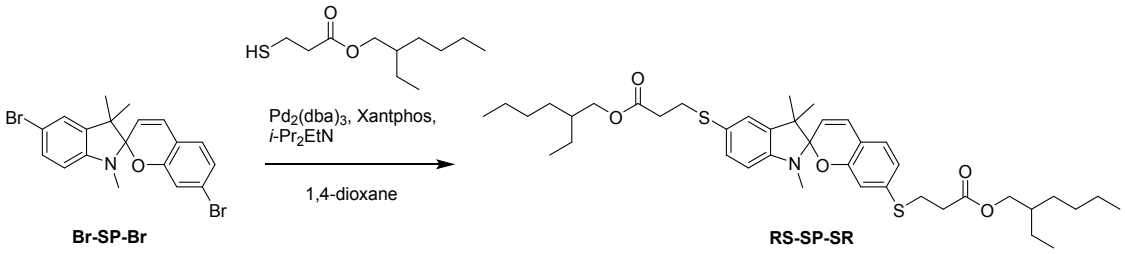

bis(2-ethylhexyl) 3,3'-((1',3',3'-trimethylspiro[chromene-2,2'-indoline]-5',7-diyl)bis(sulfanediyl))dipropionate (RS-SP-SR)

Br-SP-Br (198 mg, 0.46 mmol), 2-Ethylhexyl-3-Mercaptopropionate (221 μL, 0.97 mmol), $Pd_2(dba)_3$•$CHCl_3$ (47 mg, 0.045 mmol), Xantphos (53 mg, 0.092 mmol) and diisopropylethylamine (327 μL, 1.88 mmol) were dissolved in 3.0 mL of dry 1,4-dioxane. The mixture was refluxed overnight, following which it was washed with water and brine and dried with Na_2SO_4. The organic solvent was evaporated, and the residue was purified by column chromatography (silica-gel, Ethylacetate/hexane = 1/4) to afford 253 mg of **RS-SP-SR** in 78% yield.

^{1}H NMR (500 MHz, $CDCl_3$): δ 7.29 (dd, *J* = 8.0, 1.8 Hz, 1H), 7.15 (d, *J* = 1.8 Hz, 1H), 6.95 (d, *J* = 7.9 Hz, 1H), 6.82 (d, *J* = 10.2 Hz, 1H), 6.77 (dd, *J* = 7.9, 1.7 Hz, 1H), 6.69 (d, *J* = 1.6 Hz, 1H), 6.45 (d, *J* = 8.0 Hz, 1H), 5.62 (d, *J* = 10.2 Hz, 1H), 4.05-3.98 (m, 4H), 3.12 (t, *J* = 7.4 Hz, 2H), 3.04 (t, *J* = 7.4 Hz, 2H), 2.72 (s, 3H), 2.61 (m, 4H), 1.59-1.54 (m, 2H), 1.40-1.24 (m, 19H), 1.15 (s, 3H), 0.91-0.85 (m, 12H).

^{13}C NMR (126 MHz, CDCl3): δ 172.4, 171.9, 154.7, 148.3, 138.0, 137.6, 133.6, 129.2, 127.16, 127.12, 122.9, 120.6, 118.7, 117.0, 114.8, 107.3, 104.7, 67.35, 67.22, 51.9, 38.89, 38.84, 35.0, 34.4, 32.1, 30.55, 30.52, 29.07, 29.04, 29.01, 28.3, 26.0, 23.95, 23.90, 23.12, 23.09, 20.2, 14.21, 14.19, 11.15, 11.12.

HRMS-TOF(ESI): m/z calc.: 732.3732 $[C_{41}H_{59}NO_5S_2 + Na]^+$, found: 732.3745.

Sample preparation for BJ measurements

To a solution of **RS-SP-SR** (2.1 mg, 0.0029 mmol) in THF (0.3 mL), four equivalents of sodium ethoxide in ethanol (100 mM) were added and stirred for two hours at room temperature to deprotect

the 2-ethylhexyl-3-propionate group. Further, toluene with 4.8 equivalents of 18-crown-6 was added to make concentration of spiropyran solution 1 mM (precipitation of the spiropyran sodium salt occurred without crown ether).

STM-BJ-method procedure

The procedures applied for the STM-BJ method were in accordance with our previous work.[4]

A substrate (100-nm-thick gold films on mica annealed by butane flame) was immersed in the above-described spiropyran solution for more than an hour. Prior to break junction measurement, the substrate was washed with toluene.

STM-BJ measurements were performed using PicoSPM (Molecular Imaging) regulated by the *I-S* spectroscopy function implemented in PicoScan5 software. The STM-tip electrodes were freshly cut gold wires (0.25 mm in diameter, 99.99%). As per the STM-tip approach, the substrate surface was imaged by STM in the constant current mode confirming a clean gold surface and sharp tip. The tip was positioned on a large terrace; the STM feedback loop was switched off, and the tip was driven to contact the substrate forming a junction at a sweep rate of 50 nm/s. The tip was then retracted to break contact. During the retraction process, the current-distance traces were recorded. When molecule bridges between electrodes and maintains for a while, current value is kept constant and a plateau is shown in the traces. By making histogram with these traces, plateaus will provide peaks in the histogram and these peaks are corresponding single-molecule conductance.[5] The process of junction formation and breakage was repeated approximately ten thousand times for statistical analysis. Conductance traces having a plateau more than 0.25 nm were used to make histogram. This length criterion of 0.25 nm was stricter than reported one[6] (0.05 nm)

MCBJ-method procedure

A gold bridge was prepared by using lithography technique and plating on polyimide-covered phosphor-bronze substrate. The above-described spiropyran solution above was dropped at a point where the gold bridge was formed. After five minutes, the droplet was removed, and the substrate was dried under vacuum (Figure S1).

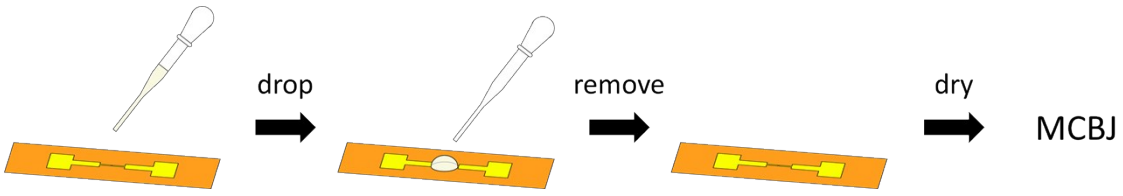

Figure S1. Sample preparation procedure for MCBJ measurement.

In MCBJ method, the substrate was bent by moving up pushing rod as shown in Fig. 1 and metal

contact will be broken. In this time, a molecule can bridge between electrodes occasionally and metal-molecule-metal junction will be formed. During metal-molecule-metal junction is maintained, I-V curves can be recorded by sweeping voltages. MCBJ measurements were then performed at 100 K in the absence of light. Further details of the machine setup for the MCBJ method are presented in our previous work.[7]

NEGF-DFT calculation

The transport properties of the molecules were calculated using SMEAGOL code[8-10] based on the SIESTA package[11]. SMEAGOL employs the non-equilibrium Green's function (NEGF) method combined with density functional theory (DFT). A double zeta plus polarization (DZP) and double zeta plus polarization (DZP) basis set were used for Au and other atoms, respectively.. The core electrons were described by the Troullier–Martins norm-conserving pseudopotential with a Kleinman–Bylander nonlocal projector. The Perdew–Burke–Ernzerhof (PBE)[12] exchange-correlation functional was used. The electrode was modelled as an Au (111) slab with a periodicity of p (5 × 5). The k points were sampled with 2 × 2 × 1 and 8 × 8 × 1 uniform grids for a self-consistent field loop and transmission coefficient, respectively. The current-voltage (*I–V)* characteristics were calculated self-consistently for each bias voltage.

Figure S2 depicts the transmission functions of the SP and MC forms calculated by the NEGF-DFT method. For the SP form, a peak corresponding to the HOMO is located at approximately −0.5 eV against the Fermi energy. On the other hand, the peak corresponding to the lowest unoccupied molecular orbital (LUMO) is located over 2.0 eV. Hence, the HOMO is closer to the Fermi energy than the LUMO, and HOMOs are dominant in the charge transport through the SP form. In addition, HOMO-1 is located immediately below HOMO. As shown in figure S3, these two orbitals move along with the electrode bias voltage. At negative bias, the HOMO approaches the Fermi level, providing larger current. On the other hand, at positive bias, the resonance between HOMO and HOMO-1 induces a minor increase in current.[13] For the MC form, the HOMO and LUMO are located at almost the same positions (approximately ±1 V) from Fermi energy. Thus, the HOMOs as well as LUMOs contribute to charge transport through the MC form. Because these orbitals are delocalized, the MC form does not exhibit rectification behavior.

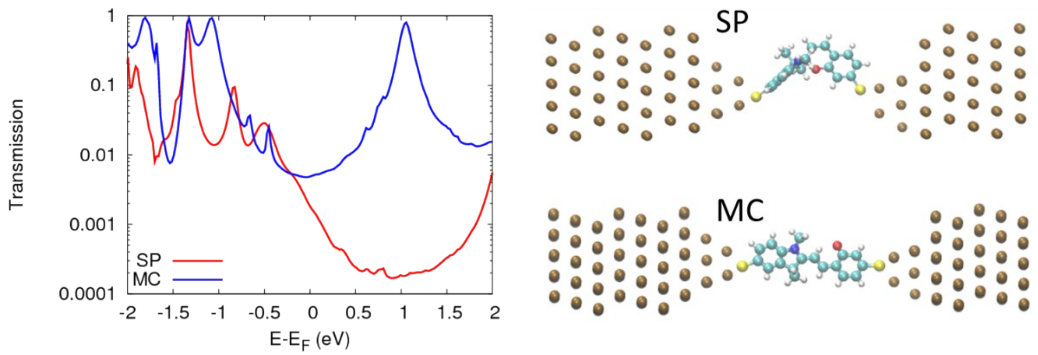

Figure S2. Calculated transmission functions of the Au-S-SP-S-Au and Au-S-MC-S-Au junctions along with the unit-cell structures employed for NEGF-DFT calculations.

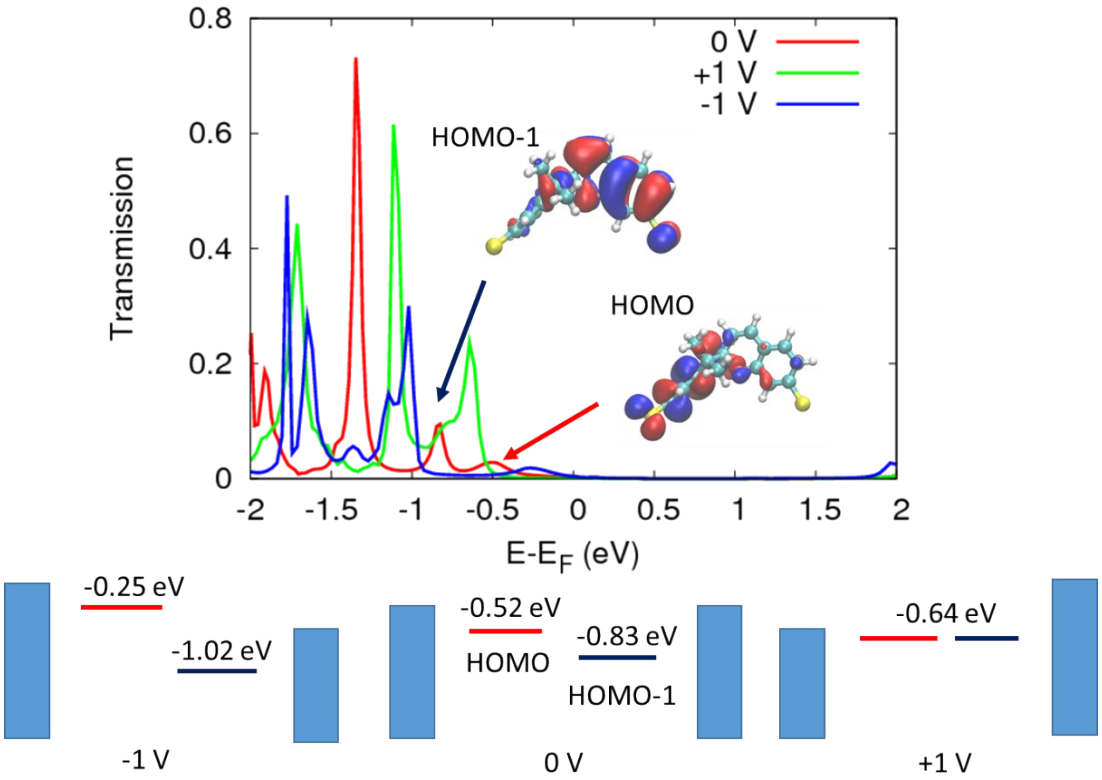

Figure S3. Voltage-dependent transmission functions of Au-S-SP-S-Au and the energy diagram of HOMO and HOMO-1 extracted from the transmission peak. The wavefunctions of HOMO and HOMO-1 at 0 V are also depicted.

Junction formation probabilities

The ratio of the junction formation probabilities of the SP and MC forms in STM-BJ was estimated using the ratio of the integration values of the fitted Gaussian function (figure S4). The resultant

ratio was SP:MC = 1:1.8, and the probability of MC was lower than that of SP, even in the STM-BJ measurements. On the other hand, in the MCBJ measurements, the junction formation probability of Au-S-MC-S-Au (~1.9%) was lower than that of Au-S-SP-S-Au (~4.6%). It was reported that the spiropyran molecule assumes an SP form at low temperatures (240 K) and MC form at high temperatures (300 K) on an Au substrate.[14] In our experiments, STM-BJ and MCBJ were performed at approximately 300 K and 100 K, respectively. Thus, it appears that considerable quantities of MC and SP forms were present in the STM-BJ and MCBJ measurements, respectively, and the existence ratio was reversed.

(a)

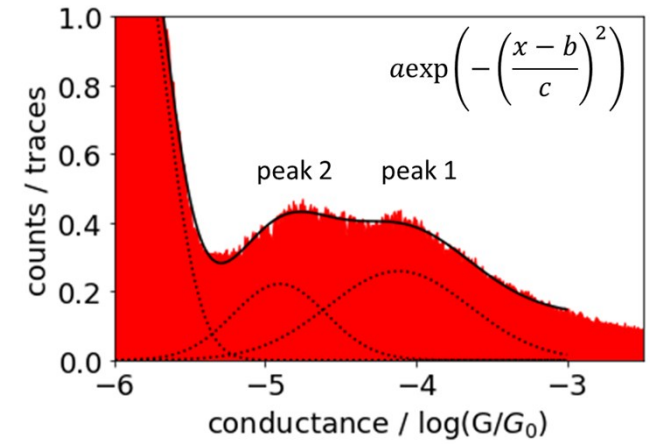

(b)

	peak 2 SP form	peak 1 MC form
a	0.259004	0.22171
b	-4.11479	-4.90144
c	0.66152	0.434615
I	0.170791	0.303686

Figure S4. (a) Fitting curves with a Gauss function for the 1D conductance histogram measured using the BJ technique and (b) summary of the fitted parameters. The integration value I of the Gaussian function was calculated as $ac\sqrt{\pi}/2$.

Other figures

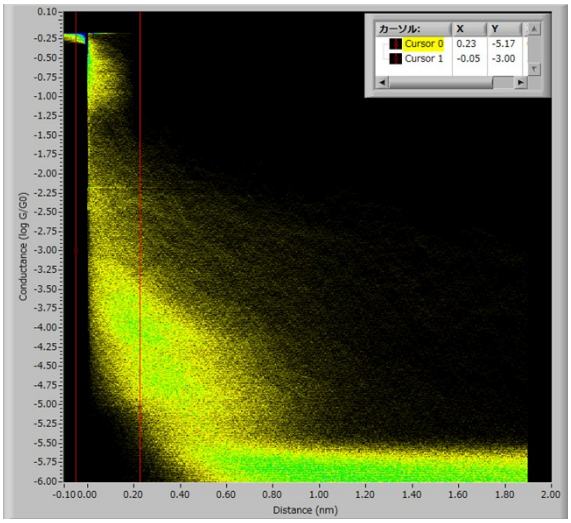

Figure S5. 2-D histogram of conductance traces of spiropyran solution recorded by STM-BJ measurement. Approximately 40 % of selected conductance traces from ten thousand traces having a plateau more than 0.25 nm were used.

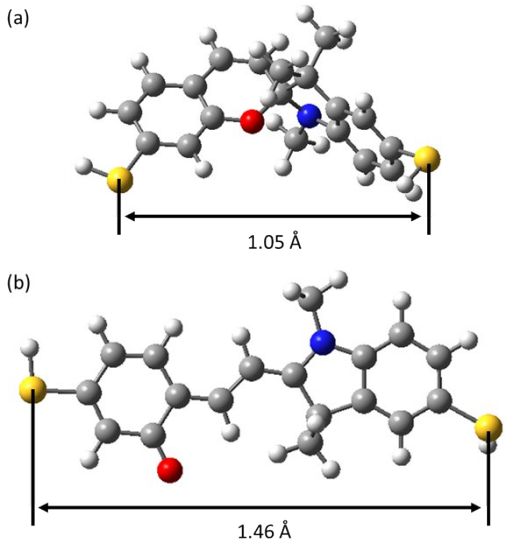

Figure S6. S-S distance of (a) HS-SP-SH and (b) HS-MC-SH in optimized structure calculated by DFT method (B3LYP/6-31g(d)).

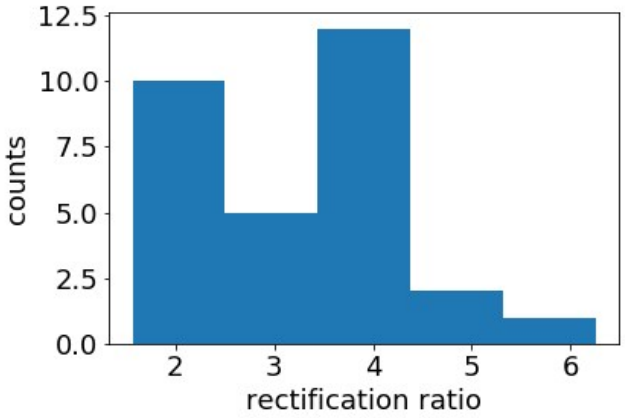

Figure S7. Histogram of rectification ratio at ±1.5 V obtained from I-V curves showing rectification of both positive and negative (total 32 curves). The average RR value was 3.3.

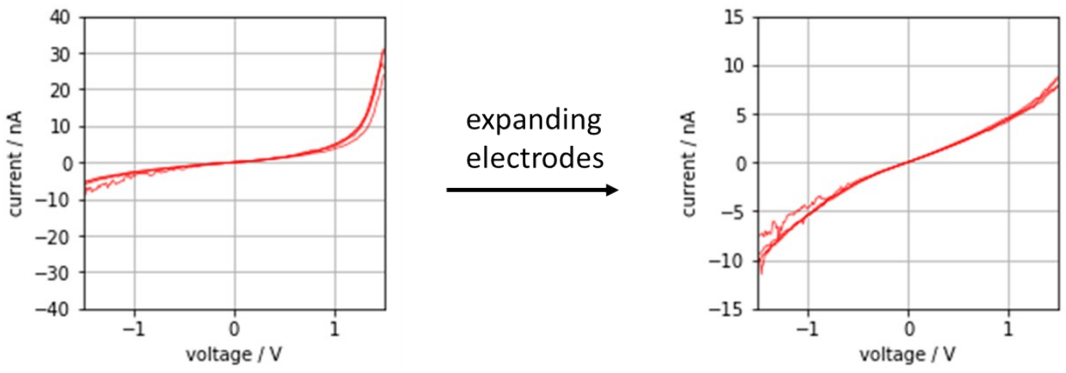

Conductance values at 200 mV

$3.0 \times 10^{-5}\ G_0$ $5.0 \times 10^{-5}\ G_0$

Figure S8. Another example of switching behavior of I-V curves from rectified to symmetric. In this molecular bridge, conductance jump was also observed by expanding electrode gap.

NMR spectra

^{1}H NMR of Br-SP-Br

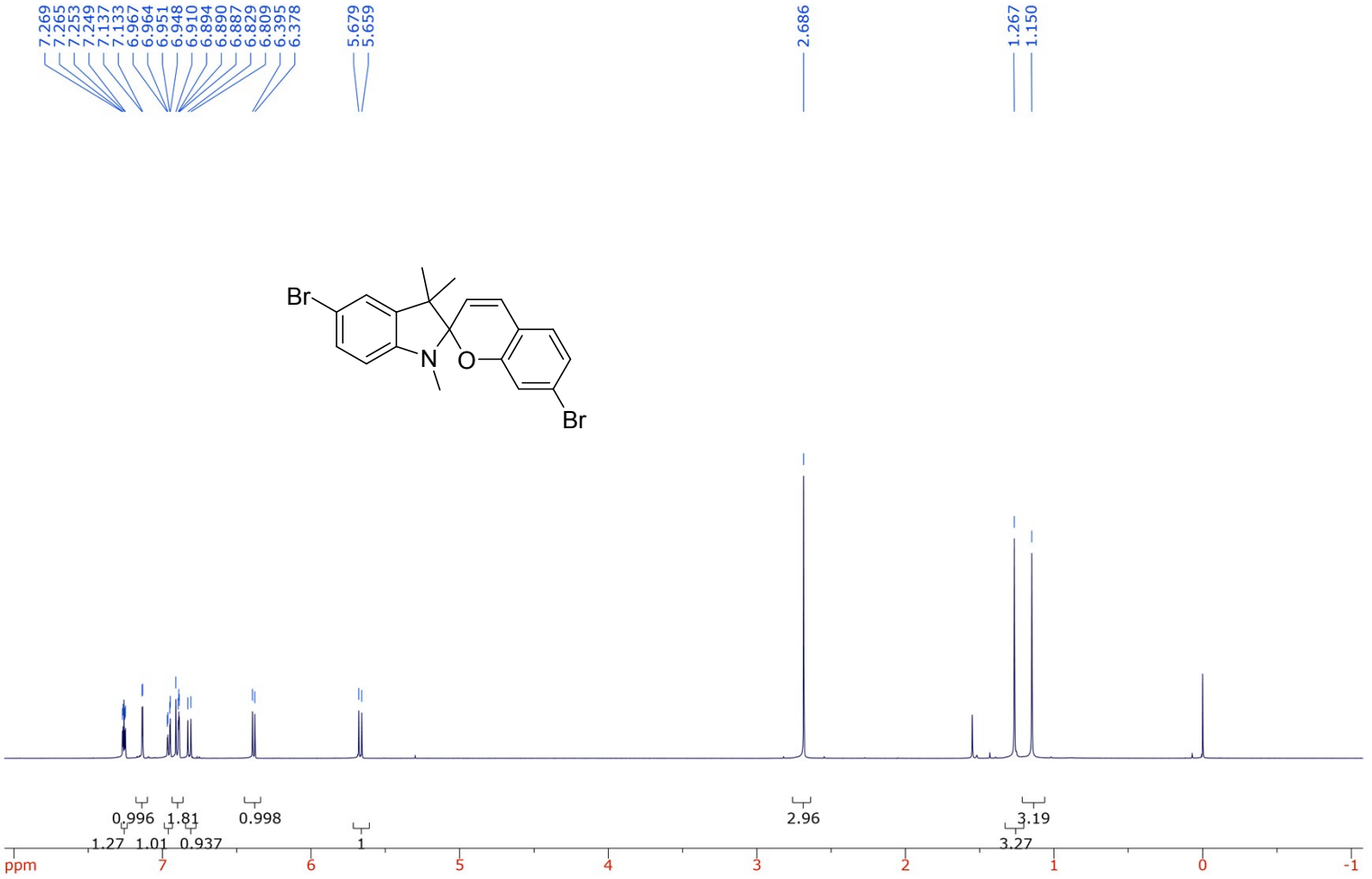

13C NMR of Br-SP-Br

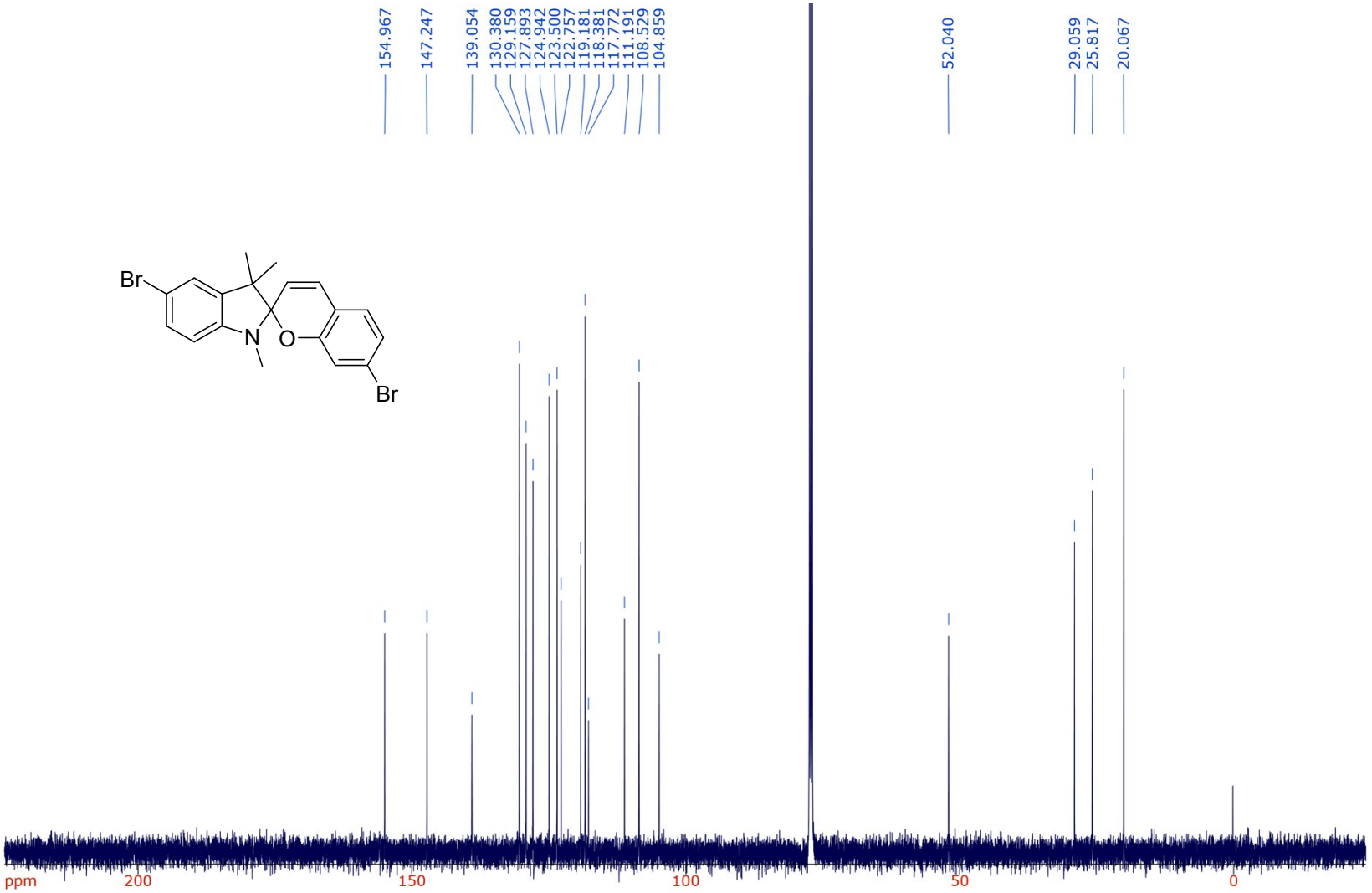

1H NMR of RS-SP-SR

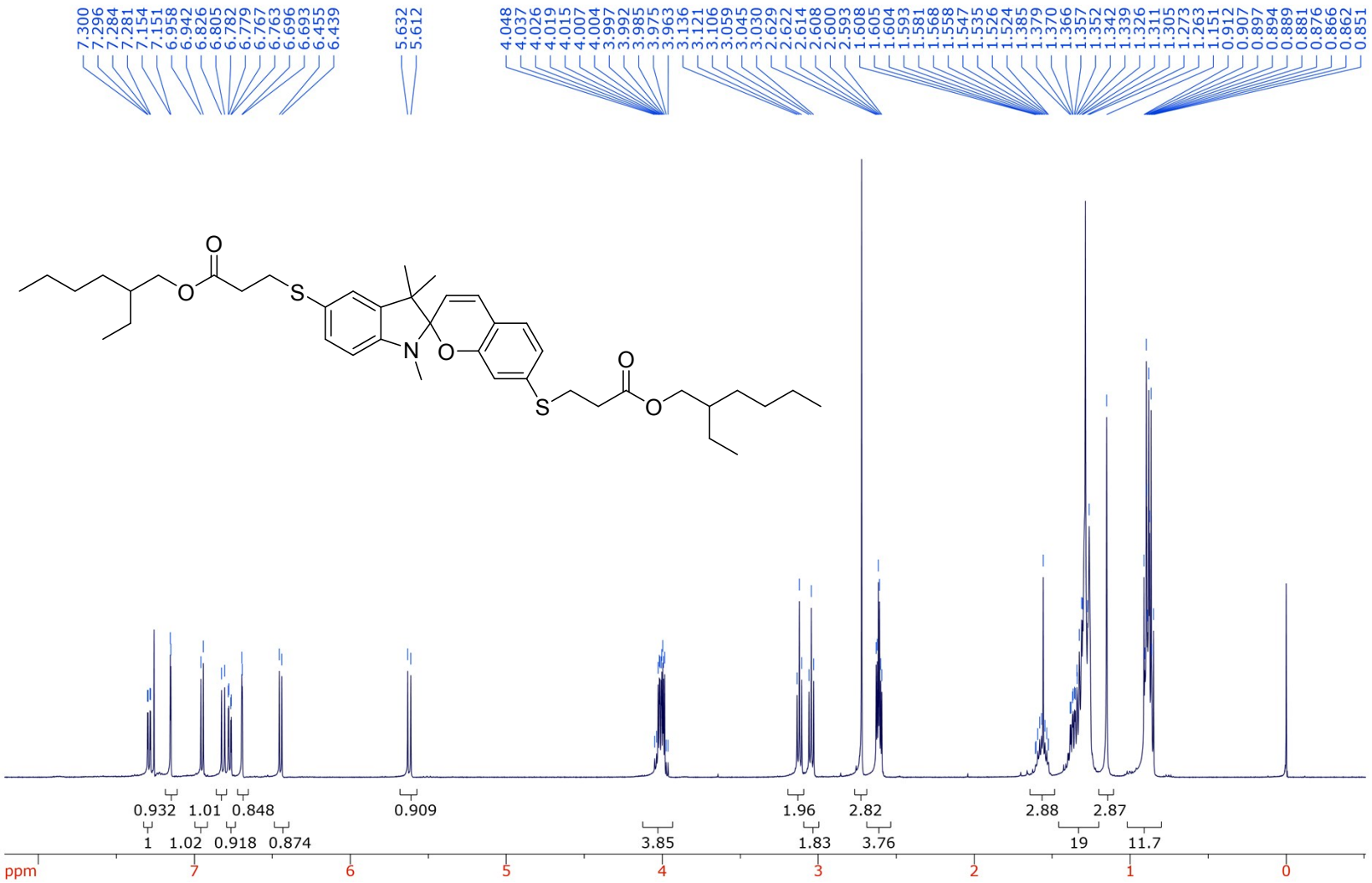

13C NMR of RS-SP-SR

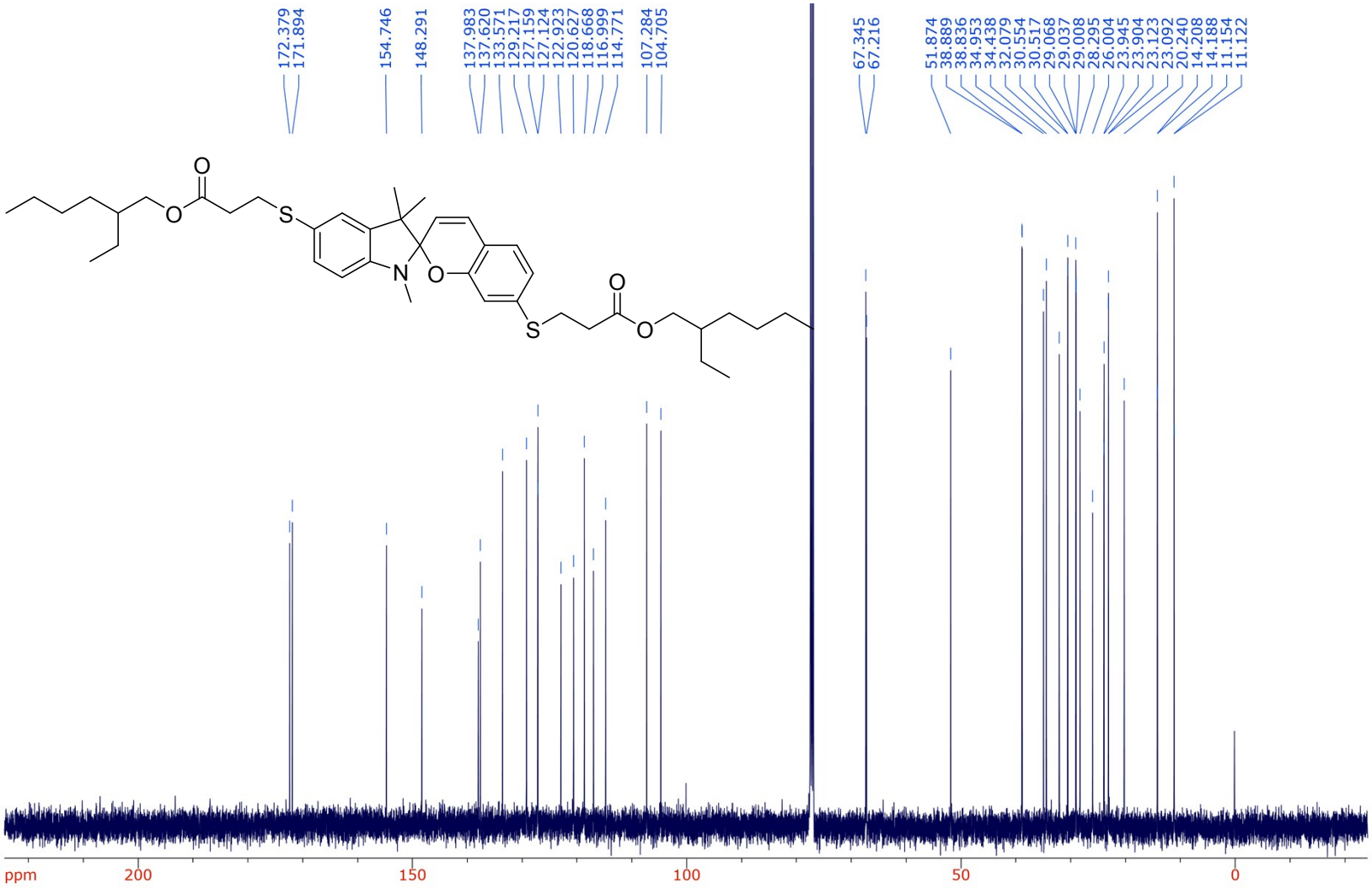

References

1. A. B. Pangborn, M. A. Giardello, R. H. Grubbs, R. K. Rosen and F. J. Timmers, *Organometallics*, 1996, **15**, 1518-1520.
2. E. A. Owens, N. Bruschi, J. G. Tawney and M. Henary, *Dyes Pigm.*, 2015, **113**, 27-37.
3. K. Matsumura, M. Ono, A. Kitada, H. Watanabe, M. Yoshimura, S. Iikuni, H. Kimura, Y. Okamoto, M. Ihara and H. Saji, *J. Med. Chem.*, 2015, **58**, 7241-7257.
4. T. Tamaki, T. Ohto, R. Yamada, H. Tada and T. Ogawa, *ChemistrySelect*, 2017, **2**, 7484-7488.
5. B. Xu and N. J. Tao, *Science*, 2003, **301**, 1221-1223.
6. Z. Li, H. Li, S. Chen, T. Froehlich, C. Yi, C. Schönenberger, M. Calame, S. Decurtins, S.-X. Liu and E. Borguet, *J. Am. Chem. Soc.*, 2014, **136**, 8867-8870.
7. R. Yamada, K. Albrecht, T. Ohto, K. Minode, K. Yamamoto and H. Tada, *Nanoscale*, 2018, **10**, 19818-19824.
8. A. R. Rocha, V. M. García-Suárez, S. Bailey, C. Lambert, J. Ferrer and S. Sanvito, *Phys.Rev. B*, 2006, **73**, 085414.
9. I. Rungger and S. Sanvito, *Phys.Rev. B*, 2008, **78**, 035407.
10. T. Ohto, I. Rungger, K. Yamashita, H. Nakamura and S. Sanvito, *Phys.Rev. B*, 2013, **87**, 205439.
11. J. M. Soler, E. Artacho, J. D. Gale, A. García, J. Junquera, P. Ordejón and D. Sánchez-Portal, *J. Phys.: Condens. Matter*, 2002, **14**, 2745-2779.
12. J. P. Perdew, K. Burke and M. Ernzerhof, *Phys. Rev. Lett.*, 1996, **77**, 3865-3868.
13. M. L. Perrin, E. Galan, R. Eelkema, F. Grozema, J. M. Thijssen and H. S. J. van der Zant, *J. Phys. Chem. C*, 2015, **119**, 5697-5702.
14. M. Piantek, G. Schulze, M. Koch, K. J. Franke, F. Leyssner, A. Krüger, C. Navío, J. Miguel, M. Bernien, M. Wolf, W. Kuch, P. Tegeder and J. I. Pascual, *J. Am. Chem. Soc.*, 2009, **131**, 12729-12735.